Learning Hierarchical Acquisition Functions for Bayesian Optimization

Nils Rottmann[1], Tjaša Kunavar[2], Jan Babič[2], Jan Peters[3,4] and Elmar Rueckert[1]

***Abstract*— Learning control policies in robotic tasks requires a large number of interactions due to small learning rates, bounds on the updates or unknown constraints. In contrast humans can infer protective and safe solutions after a single failure or unexpected observation. In order to reach similar performance, we developed a hierarchical Bayesian optimization algorithm that replicates the cognitive inference and memorization process for avoiding failures in motor control tasks. A Gaussian Process implements the modeling and the sampling of the acquisition function. This enables rapid learning with large learning rates while a mental replay phase ensures that policy regions that led to failures are inhibited during the sampling process. The features of the hierarchical Bayesian optimization method are evaluated in a simulated and physiological humanoid postural balancing task. The method outperforms standard optimization techniques, such as Bayesian Optimization, in the number of interactions to solve the task, in the computational demands and in the frequency of observed failures. Further, we show that our method performs similar to humans for learning the postural balancing task by comparing our simulation results with real human data.**

I. INTRODUCTION

Autonomous systems such as anthropomorphic robots or self-driving cars must not harm cooperating humans in co-worker scenarios, pedestrians on the road or them selves. To ensure safe interactions with the environment state-of-the-art robot learning approaches are first applied to simulations and afterwards an expert selects final candidate policies to be run on the real system. However, for most autonomous systems a fine-tuning phase on the real system is unavoidable to compensate for unmodelled dynamics, motor noise or uncertainties in the hardware fabrication.

Several strategies were proposed to ensure safe policy exploration. In special tasks like in robot arm manipulation the operational space can be constrained, for example, in classical null-space control approaches [1]–[6] or constraint black-box optimizer [7]–[11]. While this null-space strategy works in controlled environments like research labs where the environmental conditions do not change, it fails in everyday life tasks as in humanoid balancing where the priorities or constraints that lead to hardware damages when falling are unknown.

Alternatively, limiting the policy updates by applying probabilistic bounds in the robot configuration or motor command space [12]–[16] were proposed. These techniques do not assume knowledge about constraints. Closely related are also Bayesian optimization techniques with modulated acquisition functions [17]–[20] to avoid exploring policies that might lead to failures. However, all these approaches do not avoid failures but rather an expert interrupts the learning process when it anticipates a potential dangerous situation.

All the aforementioned strategies cannot avoid harming the system itself or the environment without thorough experts knowledge, controlled environmental conditions or human interventions. As humans require just few trials to perform reasonably well, it is desired to enable robots to reach similar performance even for high-dimensional problems. Thereby, most approaches are based on the assumption of a "low effective dimensionality", thus most dimensions of a high-dimensional problem do not change the objective function significantly. In [21] a method for relevant variable selection based on Hierarchical Diagonal Sampling for both, variable selection and function optimization, has been proposed. Randomization combined with Bayesian Optimization is proposed in [22] to exploit effectively the aforementioned "low effective dimensionality". In [23] a dropout algorithm has been introduced to overcome the high-dimensionality problem by only train onto a subset of variables in each iteration, evaluating a "regret gap" and providing strategies

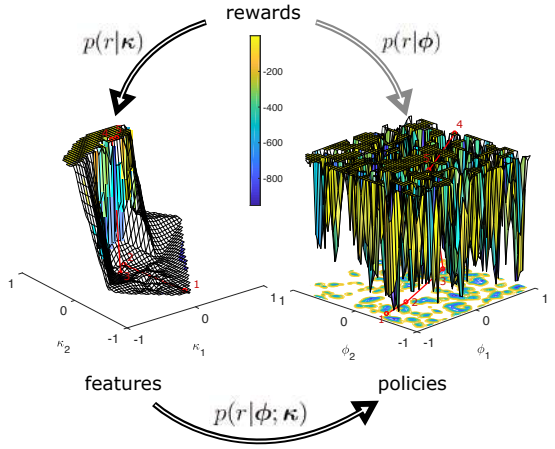

Fig. 1: Illustration of the hierarchical BO algorithm. In standard BO (clock-wise arrow), a mapping from policy parameters to rewards is learned, i.e., $\boldsymbol{\phi} \mapsto r \in \mathbb{R}^1$. We propose a hierarchical process, where first features $\boldsymbol{\kappa}$ are sampled and later used to predict the potential of policies conditioned on these features, $\boldsymbol{\phi}|\boldsymbol{\kappa} \mapsto r$. The red dots show the first five successive roll-outs in the feature and the policy space of a humanoid postural control task.

[1]Institute for Robotics and Cognitive Systems, University of Luebeck, Ratzeburger Allee 160, 23562 Luebeck, Germany
[2]Neuromechanics and Biorobotics Lab at Jožef Stefan Institute, Slovenia
[3]Intelligent Autonomous Systems Lab, Technische Universität Darmstadt, Germany
[4]Robot Learning Group, Max-Planck Institute for Intelligent Systems, Tuebingen, Germany
Correspondence to rottmann@rob.uni-luebeck.de

to reduce this gap efficiently. In [24] an algorithm has been proposed which optimizes an acquisition function by building new Gaussian Processes with sufficiently large kernel-lengths scales. This ensures significant gradient updates in the acquisition function to be able to use gradient-dependent methods for optimization.

The contribution of this paper is the introduction of a hierarchical process for Bayesian Optimization (HiBO) which uses features for optimization to significantly reduce the number of required roll-outs. In feature space we search for the optimum of the acquisition function by sampling and later use the best feature configuration to optimize the policy parameters which are conditioned on the given features, see also Figure 1. We show that our approach reduces the number of required roll-outs significantly compared to standard Bayesian Optimization. Further, a second contribution of this paper is that we propose a computational model for rapid motor-adaptation performance in challenging humanoid postural control tasks [25].

During the submission of this paper, a new approach for efficiently optimizing high-dimensional Bayesian Optimization problems has been proposed [26]. There, a learning procedure based on multi-layer neural networks from the input space to a feature space and back has been proposed. The optimization happens in the feature space and afterwards a retransformation to the input space occurs. In future work, we will compare these approach with ours.

II. METHODS

In this section we introduce the methodology of our hierarchical BO approach. We start with the general problem statement and afterwards briefly summarize the concept of BO which we use here as a baseline. We then go through the basic principles required for our algorithm and finally we explain mental replay.

A. Problem Statement

The goal is to find the best policy $\pi^*(\boldsymbol{\theta}|\boldsymbol{c})$ that maximizes the return

$$J(\boldsymbol{\theta}) = \mathbb{E}\left[\sum_{t=0}^{T} \{r_t(\boldsymbol{x}_t, \boldsymbol{u}_t) \,|\, \pi(\boldsymbol{\theta}|\boldsymbol{c})\}\right] , \tag{1}$$

with reward $r_t(\boldsymbol{x}_t, \boldsymbol{u}_t)$ at time step t for executing the motor commands $\boldsymbol{u}_t$ in state $\boldsymbol{x}_t$.

For learning the policy vector and the features, we collect samples of the return $J(\boldsymbol{\theta}^{[k]}) \in \mathbb{R}^1$, the evaluated policy parameter vector $\boldsymbol{\theta}^{[k]} \in \mathbb{R}^m$ and the observed features modeled by $\boldsymbol{c}^{[k]} \in \mathbb{R}^n$. All variables used are summarized in Table I. The optimization problem is defined as

$$\langle \boldsymbol{\theta}^* \,,\, \boldsymbol{c}^* \rangle = \underset{\boldsymbol{\theta},\boldsymbol{c}}{\operatorname{argmax}} \mathbb{E}\left[\, J(\boldsymbol{\theta}) \,|\, \pi(\boldsymbol{\theta}|\boldsymbol{c}) \,\right] . \tag{2}$$

The optimal parameter vector and the corresponding feature vector can be found in an hierarchical optimization process which is discussed in Section II-C.

B. Bayesian Optimization (baseline)

Bayesian Optimization (BO) has emerged as a powerful tool to solve various global optimization problems where roll-outs are expensive and a sufficient accurate solution has to be found with only few evaluations, e.g. [27]–[29]. In this paper we use the standard BO as a benchmark for our proposed hierarchical process. Therefore, we now briefly summarize the main concept. For further details refer to [20].

The main concept of Bayesian Optimization is to build a model for a given system based on the so far observed data $D = \{X, \boldsymbol{y}\}$. The model describes a transformation from a given data point $\boldsymbol{x} \in X$ to a scalar value $y \in \boldsymbol{y}$, e.g. from the parameter vector $\boldsymbol{\theta}$ to the return $J(\boldsymbol{\theta})$. Such model can either be parametrized or non-parametrized and is used for choosing the next query point by evaluating an acquisition function $\alpha(D)$. Here, we use the non-parametric Gaussian Processes (GPs) for modeling the unknown system which are state-of-the-art model learning or regression approaches [30], [31] that were successfully used for learning inverse dynamics models in robotic applications [32], [33]. For comprehensive discussions we refer to [34], [35].

GPs represent a distribution over a partial observed system in the form of

$$\begin{bmatrix} \boldsymbol{y} \\ \boldsymbol{y}_* \end{bmatrix} \sim N\left(\begin{bmatrix} \boldsymbol{m}(X) \\ \boldsymbol{m}(X_*) \end{bmatrix}, \begin{bmatrix} \boldsymbol{K}(X,X) & \boldsymbol{K}(X,X_*) \\ \boldsymbol{K}(X_*,X) & \boldsymbol{K}(X_*,X_*) \end{bmatrix}\right), \tag{3}$$

where $D = \{X, \boldsymbol{y}\}$ are the so far observed data points and $D_* = \{X_*, \boldsymbol{y}_*\}$ the query points. This representation is fully defined by the mean $\boldsymbol{m}$ and the covariance $\boldsymbol{K}$. We chose $m(\boldsymbol{x}) = 0$ as mean function and as covariance function a *Matérn kernel* [36]. It is a generalization of the *squared-exponential kernel* that has an additional parameter ν which controls the smoothness of the resulting function. The smoothing parameter can be beneficial for learning local models. We used *Matérn kernels*

$$k(\boldsymbol{x}_p, \boldsymbol{x}_q) = \sigma^2 \, \frac{1}{2^{\nu-1}\,\Gamma(\nu)} \, A^\nu \, \mathrm{H}_\nu \, A + \sigma_y^2 \, \delta_{pq} \,,$$

with $\nu = 5/2$ and the gamma function Γ, $A = (2\sqrt{\nu}||\boldsymbol{x}_p - \boldsymbol{x}_q||)/l$ and modified *Bessel* function H_ν [37]. The length-scale parameter of the kernel is denoted by σ, the variance of the latent function is denoted by σ_y and δ_{pq} is the *Kronecker* delta function (which is one if $p = q$ and zero otherwise). Note that for $\nu = 1/2$ the

TABLE I: Variable definitions used in this paper.

$J(\boldsymbol{\theta})$	$\mathbb{R}^1$	return of a rollout
$r_t(\boldsymbol{x}_t, \boldsymbol{u}_t)$	$\mathbb{R}^1$	intermediate reward give at time t
$\boldsymbol{x}_t$	$\mathbb{R}^d$	state of the system
$\boldsymbol{u}_t$	$\mathbb{R}^l$	motor commands of the system
$\pi(\boldsymbol{\theta}\|\boldsymbol{c})$		unknown control policy
$\boldsymbol{\theta}$	$\mathbb{R}^m$	policy vector
$\boldsymbol{c}$	$\mathbb{R}^n$	feature vector
$s^{[k]}$	$\{0,\, 1\}$	flag indicating the success of rollout k

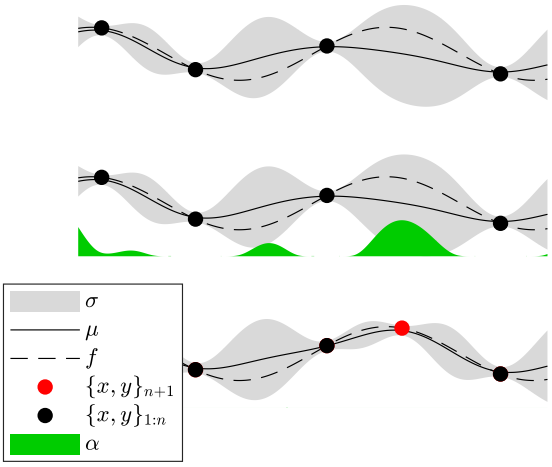

Fig. 2: Illustration of the Bayesian Optimization Process. Based on the measurements $D = \{x_{1:n}, y_{1:n}\}$ the mean $\boldsymbol{\mu}$ and variance $\boldsymbol{\sigma}$ are estimated for sampled position in a defined area (grey area). The acquisition function $\alpha(x; D)$ is calculated as in Equation (5) and the position of the maximum value $\max_x \alpha(x; D)$ is chosen as next evaluation point x_{n+1}. For comparison the true function f is depicted as dashed line.

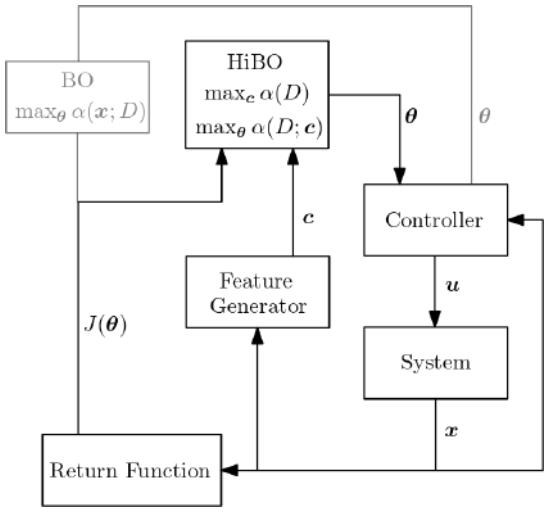

Fig. 3: Comparison between the standard Bayesian Optimization (BO) approach and the proposed hierarchical Bayesian Optimization (HiBO). The control policy, executed by the controller, is defined by the parameters $\boldsymbol{\theta}$, which have to be learned.

Matérn kernel implements the *squared-exponential kernel*. In our experiments, we optimized the hyperparameters σ, l, σ_y by maximizing the marginal likelihood [31].

Predictions for a query points $D_* = \{\boldsymbol{x}_*, y_*\}$ can then be determined as

$$\begin{aligned} \mathrm{E}(y_*|\boldsymbol{y}, X, \boldsymbol{x}_*) &= \mu(\boldsymbol{x}_*) = m_* + \boldsymbol{K}_*^\top \boldsymbol{K}^{-1}(\boldsymbol{y} - \boldsymbol{m}) \\ \mathrm{var}(y_*|\boldsymbol{y}, X, \boldsymbol{x}_*) &= \sigma(\boldsymbol{x}_*) = \boldsymbol{K}_{**} - \boldsymbol{K}_*^\top \boldsymbol{K}^{-1} \boldsymbol{K}_*. \end{aligned} \tag{4}$$

The predictions are then used for choosing the next model evaluation point $\boldsymbol{x}_n$ based on the acquisition function $\alpha(\boldsymbol{x}; D)$. We use expected improvement (EI) [38] which considers the amount of improvement

$$\begin{aligned} \alpha(\boldsymbol{x}; D) = (\mu(\boldsymbol{x}) - \tau)\, \Phi\left(\frac{\mu(\boldsymbol{x}) - (\tau + \xi)}{\sigma(\boldsymbol{x})}\right) \\ + \sigma(\boldsymbol{x}) \phi\left(\frac{\mu(\boldsymbol{x}) - (\tau + \xi)}{\sigma(\boldsymbol{x})}\right), \end{aligned} \tag{5}$$

where τ is the so far best measured value $\max(\boldsymbol{y})$, Φ the standard normal cumulative distribution function, ϕ the standard normal probability density function and $\xi \sim \sigma_\xi U(-0.5, 0.5)$ a random value to ensure a more robust exploration. Samples, distributed over the area of interest, are evaluated and the best point is chosen for evaluation based on the acquisition function values. In Figure 2 the Bayesian Optimization process is illustrated.

C. Hierarchical Sampling from Acquisition Functions in Bayesian Optimization

We learn a joint distribution $p(J(\boldsymbol{\theta}^{[k]}), \boldsymbol{\theta}^{[k]}, \boldsymbol{c}^{[k]})$ over $k = 1, ..., K$ roll-outs of observed triples. This distribution is used for as a prior of the acquisition function in Bayesian optimization. However, instead of directly conditioning on the most promising policy vectors using $\alpha_{BO} = \alpha(\boldsymbol{\theta}; D)$, we propose an iterative conditioning scheme. Therefore, the two acquisition functions

$$\alpha_{\boldsymbol{c}} = \alpha(\boldsymbol{c}; D), \tag{6}$$

$$\alpha_{\boldsymbol{\theta}} = \alpha(\boldsymbol{\theta}; \boldsymbol{c}, D), \tag{7}$$

are employed, where for Equation (7), the evaluated mean $\mu(\boldsymbol{\theta}; \boldsymbol{c})$ and variance $\sigma(\boldsymbol{\theta}; \boldsymbol{c})$ for the parameter $\boldsymbol{\theta}$ are conditioned on the features $\boldsymbol{c}$. The hierarchical optimization process works then as follows:
In the first step we estimate the best feature values based on a GP model using the acquisition function from Equation (6)

$$\boldsymbol{c}^{[k+1]} = \max_{\boldsymbol{c}} \alpha(\boldsymbol{c}; D^{[1:k]}). \tag{8}$$

These feature values are then used to condition the search for the best new parameter $\boldsymbol{\theta}^{[k+1]}$ using Equation (7)

$$\boldsymbol{\theta}^{[k+1]} = \max_{\boldsymbol{\theta}} \alpha(\boldsymbol{\theta}; \boldsymbol{c}^{[k+1]}, D^{[1:k]}). \tag{9}$$

We subsequently continue evaluating the policy vector $\boldsymbol{\theta}^{[k+1]}$ using the reward function presented in Equation (1). Finally, the new data point $\langle J(\boldsymbol{\theta}^{[k+1]}), \boldsymbol{\theta}^{[k+1]}, \boldsymbol{c}^{[k+1]} \rangle$ can be added to the set of data points D. In Figure 3 differences between standard BO and HiBO are highlighted.

D. Mental Replay

To ensure robustness for Bayesian Optimization, mental replays can be generated. Therefore, the new training data set $\langle J(\boldsymbol{\theta}^{[k+1]}), \boldsymbol{\theta}^{[k+1]}, \boldsymbol{c}^{[k+1]} \rangle$, generated by the policy parameter $\boldsymbol{\theta}^{[k+1]}$, will be enlarged by augmenting perturbed

Algorithm 1 Hierarchical Acquisition Function Sampling for Bayesian Optimization (HiBO)

1: Initialize the dataset $D^{[1:k]} = \langle J(\boldsymbol{\theta}^{[k]}), \boldsymbol{\theta}^{[k]}, \boldsymbol{c}^{[k]} \rangle$ with K rollouts of sampled policies $\boldsymbol{\theta}$.
2: **for** k = K, K+1, ... **do**
3: $\quad \boldsymbol{c}^{[k+1]} = \text{argmax}_{\boldsymbol{c}}\, \alpha(D^{[1:k]}) \,:\, D \rightarrow \mathbb{R}^1$ using Eq. 6.
4: $\quad \boldsymbol{\theta}^{[k+1]} = \text{argmax}_{\boldsymbol{\theta}}\, \alpha(D^{[1:k]}; \boldsymbol{c}^{[k+1]})$ using Eq. 7.
5: $\quad$ Evaluate the policy vector $\boldsymbol{\theta}^{[k+1]}$ using Eq. 1.
6: $\quad$ Augment $D = [D^{[1:k]}, \langle J(\boldsymbol{\theta}^{[k+1]}), \boldsymbol{\theta}^{[k+1]}, \boldsymbol{c}^{[k+1]} \rangle^l]$.
7: **end for**

copies of the policy parameter $\boldsymbol{\theta}^{[k+1]}$. These l copies are then used for generating the augmented training data sets

$$D^{[k+1]} = \langle J(\boldsymbol{\theta}^{[k+1]}), \boldsymbol{\theta}^{[k+1]}, \boldsymbol{c}^{[k+1]} \rangle^l. \tag{10}$$

Here, the transcript $\langle \cdot \rangle^l$ denotes l perturbed copies of the given set. Hence, perturbed copies of the parameters $\boldsymbol{\theta}^{[k+1]}$ and features $\boldsymbol{c}^{[k+1]}$ are generated keeping the objective $J(\boldsymbol{\theta}^{[k+1]})$ constant. In Algorithm (1) the complete method is summarized. We evaluate different replay strategies in the result Section in III-C.

III. RESULTS

In this section we first present observations on human learning during perturbed squat-to-stand movements. We compare the learning results of a simulated humanoid to the learning rates achieved by the human participants. Second, we evaluate our hierarchical BO approach in comparison to our baseline, the standard BO. Third we evaluate the impact of mental replays on the performance of our algorithm.

A. Human postural balancing

To observe human learning, we designed an experiment where 20 male participants were subjected to waist pull perturbation during squat-to-stand movements, see Figure 4. Participants had to stand up from a squat position without making any compensatory steps (if they made a step, such trial was considered a fail). Backward perturbation to the centre of mass (CoM) was applied by a pulling mechanism and was dependent on participants' mass and vertical CoM velocity.

Fig. 4: Experimental setup for the squat-to-stand movements.

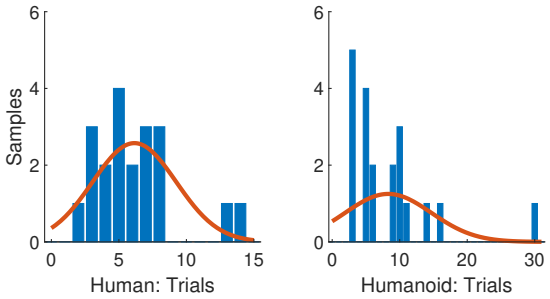

Fig. 5: Histogram showing the number of required trials until the first successful episode for both, the human experiments and the simulated humanoid, with $\mu_{\text{human}} = 6.15$, $\sigma_{\text{human}} = 3.1$, $\mu_{\text{humanoid}} = 8.3$ and $\sigma_{\text{humanoid}} = 6.38$.

On average, participants required 6 trials ($\sigma_{\text{human}} = 3.1$) to successfully complete the motion. On the left panel of Figure 5, a histogram of the required trials before the first success is shown. On the right panel, the evaluation results for the simulated humanoid are presented (details on the implementation are discussed in the subsequent Subsection III-B). The human learning behavior is faster and more reliable than the learning behavior of the humanoid. However, humans can exploit fundamental knowledge about whole body balancing whereas our humanoid has to learn everything from scratch. Only the gravity constant was set to zero in our simulation, as we are only interested in the motor adaptation and not in gravity compensation strategies.

Adaptation was evaluated using a measure based on the trajectory area (TA) at every episode as defined in [39]. The Trajectory area represents the total deviation of the CoM trajectory with respect to a straight line. The trajectory area of a given perturbed trajectory is defined as the time integral of the distance of the trajectory points to the straight line in the sagittal plane:

$$TA(e_x) = \int_{t_0}^{t_{end}} x(t)|\dot{y}(t)|\mathrm{d}t \tag{11}$$

A positive sign represents the anterior direction while a negative sign represents the posterior direction. The mean and standard deviation for the trajectory area over the number of training episodes for all participants are depicted in Figure 6. Comparing these results with the simulation results of our humanoid shows that the learning rate using our approach is similar to the learning rate of real humans.

B. Humanoid postural balancing

To test the proposed algorithm we simulated a humanoid postural control task as shown in Figure 7. The simulated humanoid has to stand up and is thereby exposed to an external pertubation proportional to the velocity of the CoM in the superior direction in the sagittal plane. The pertubation is applied during standing up motion such that the robot has to learn to counter balance. The simulated humanoid consist of four joints, connected by rigid links, where the

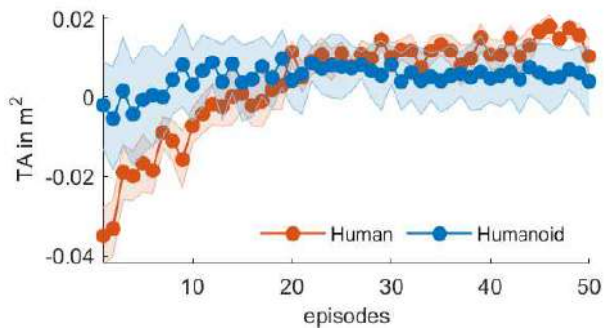

Fig. 6: Mean and standard deviaton of the trajectory area (TA) with regard to the number of episodes for both, the human experiments and the simulated humanoid. For the humanoid the x-coordinates have been shifted about -0.5 to account for the stretched arms. In addition, the trajectory area of the humanoid has been scaled with the factor 0.1 and shifted about -0.2 to allow easier comparison.

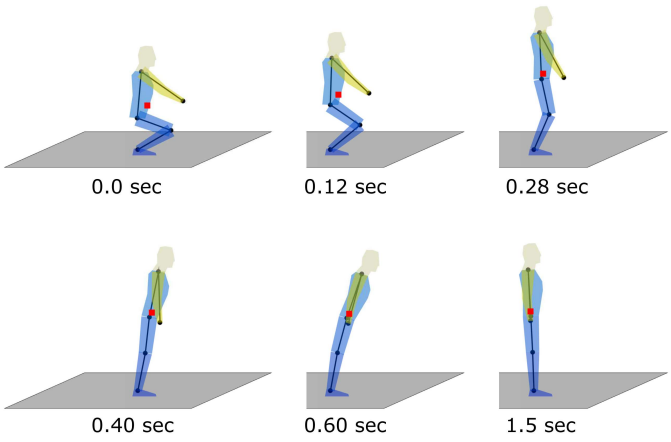

Fig. 7: Illustration of the humanoid postural control task. An external perturbation is applied during the standing up motion and the robot has to learn to counter balance. The perturbation is proportional to the CoM velocity in the superior direction in the *sagittal plane*.

position of the first joint is fixed onto the ground. A PD-controller is used with $K_{P,i}$ and $K_{D,i}$ for $i = 1, 2, 3, 4$ being the proportional and derivative gains. In our simulations the gains are set to $K_{P,i} = 400$ and $K_{D,i} = 20$ and an additive control noise $\epsilon \sim \mathcal{N}(0, 1)$ has been inserted such that the control input for a certain joint becomes

$$u_i = K_{P,i}\ e_{P,i} + K_{D,i}\ e_{D,i} + \epsilon, \tag{12}$$

where $e_{P,i}$, $e_{D,i}$ are the joint errors regarding the target position and velocity. The control gains can also be learned. The goal positions and velocities for the joints are given. As parametrized policy, we use a via point $[\phi_i, \dot{\phi}_i]$, where ϕ_i is the position of joint i at time t_{via} and $\dot{\phi}_i$ the corresponding velocity. Hence, the policy is based on 9, respectively 17 parameters (if the gains are learned), which are summarized in Table II. For our simulations we handcrafted 7 features, namely the overall success, the maximum deviation of the CoM in x and y direction and the velocities of the CoM for the x and y directions at $200\,ms$ respectively $400\,ms$. In Table III the features used in this paper are summarized. Simultaneously learning of the features is out of scope of this comparison to human motor performance but part of future work.

We simulated the humanoid in each run for a maximum of $t_{\max} = 2\,s$ with a simulation time step of $\mathrm{d}t = 0.002\,s$, such that a maximum of $N = 1000$ simulation steps are used. The simulation has been stopped at the simulation step N_{end} if either the stand up has been failed or the maximum simulation time has been reached. The return of a roll-out $J(\boldsymbol{\theta})$ is composed according to

$$J(\boldsymbol{\theta}) = -(c_{\text{balance}} + c_{\text{time}} + c_{\text{control}}) \tag{13}$$

with the balancing costs

$$c_{\text{balance}} = \frac{1}{N_{\text{end}}} \sum_{i=1}^{N_{\text{end}}} ||\boldsymbol{x}_{\text{CoM,target}} - \boldsymbol{x}_{\text{CoM,i}}||^2, \tag{14}$$

the time costs

$$c_{\text{time}} = (N - N_{\text{end}}), \tag{15}$$

and the control costs

$$c_{\text{control}} = 10^{-8} \sum_{i=1}^{N_{\text{end}}} \sum_{j=1}^{4} u_{ij}^2. \tag{16}$$

We compared our approach with our baseline, standard Bayesian Optimization. For that we used the features $4, 5$ in III and set the number of mental replays to $l = 3$. We initialized both, the BO and the HiBO approach with 3 seed points and generated average statistics over 20 runs. In Figure 8 the comparison between the rewards of the algorithms over 50 episodes is shown. In Figure 9 (a) the number of successful episodes is illustrated. Our approach requires significantly fewer episodes to improve the reward then standard Bayesian Optimization (10 ± 3 vs 45 ± 5) and has a higher success quote ($78\% \pm 24\%$ vs $60\% \pm 7\%$).

We further evaluated the impact of the different features on the learning behavior. In Figure 9 (b) the average statistics

TABLE II: Policy parameter description

$K_{P,i}$	proportional gain for joint i
$K_{D,i}$	derivative gain for joint i
ϕ_i	angle of joint i at the via point
$\dot{\phi}_i$	angular velocity of joint i at the via point
t_{via}	time for switching from the via point to goal position

TABLE III: Feature description

Feature 1	success
Feature 2	maximum deviation of the CoM in x direction
Feature 3	maximum deviation of the CoM in y direction
Feature 4	velocity of the CoM in x direction at $200\,ms$
Feature 5	velocity of the CoM in y direction at $200\,ms$
Feature 6	velocity of the CoM in x direction at $400\,ms$
Feature 7	velocity of the CoM in y direction at $400\,ms$

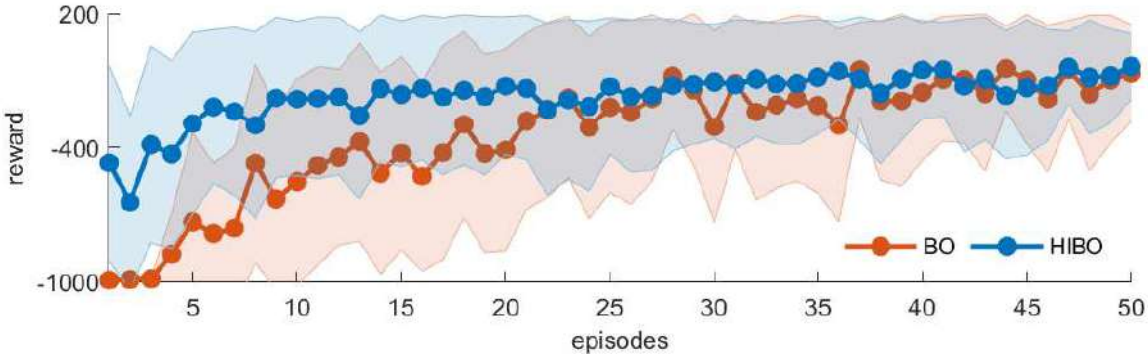

Fig. 8: Comparison of the rewards of the proposed *HIBO* algorithm and the state-of-the-art approach *Bayesian Optimization*. Shown are average statistics (mean and standard deviation) over 20 runs.

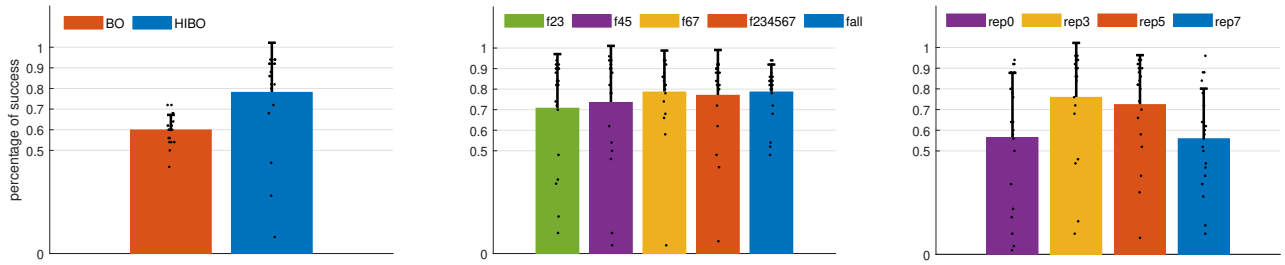

(a) (b) (c)

Fig. 9: Comparison of the number of successful episodes of the proposed *HIBO* algorithm and the state-of-the-art approach *Bayesian Optimization* for different internal experience replay iterations. The last three algorithms implemented an *automatic relevance determination* of the *Gaussian Process* features and policy parameters. Shown are average statistics (mean and standard deviation) over 20 runs and the true data values are denoted by the black dots.

over 20 runs for different selected features with 3 mental replays are shown. All feature pairs generate better results on average then standard BO, whereas for the evaluated task no significant difference in the feature choice was observed.

C. Exploiting Mental Replays

We evaluated our approach with additional experience replays. For that we included an additive noise of $\epsilon_{\text{rep}} \sim \mathcal{N}(0, 0.05)$ to perturb the policy parameters and features. In Figure 9 (c) average statistics over 20 runs of the success rates for different number of replay episodes are shown (rep3 = 3 replay episodes). Our proposed algorithm works best with a number of 3 replay episodes. Five or more replays in every iteration steps even reduce the success rate of the algorithm.

IV. CONCLUSION

We introduced HiBO, a hierarchical approach for Bayesian Optimization. We showed that HiBO outperforms standard BO in a complex humanoid postural control task. Moreover, we demonstrated the effects of the choice of the features and for different number of mental replay episodes. We compared our results to the learning performance of real humans at the same task. We found that the learning behavior is similar. We found that our proposed hierarchical BO algorithm can reproduce the rapid motor adaptation of human subjects. In contrast standard BO, our comparison method, is about four times slower. In future work, we will examine the problem of simultaneously learning task relevant features in neural nets.

V. ACKNOWLEDGEMENT

This project has received funding from the European Union's Horizon 2020 research and innovation programme under grant agreement No #713010 (GOAL-Robots), No #640554 (SKILLS4ROBOTS) and by the Deutsche Forschungsgemeinschaft (DFG, German Research Foundation) - No #430054590 (TRAIN).

REFERENCES

[1] P. Baerlocher and R. Boulic, "Task-priority formulations for the kinematic control of highly redundant articulated structures." in *IROS*, 1998, pp. 13–17.

[2] S. B. Slotine, "A general framework for managing multiple tasks in highly redundant robotic systems," in *proceeding of 5th International Conference on Advanced Robotics*, vol. 2, 1991, pp. 1211–1216.

[3] S. I. Choi and B. K. Kim, "Obstacle avoidance control for redundant manipulators using collidability measure," *Robotica*, pp. 143–151, 2000.

[4] M. Gienger, H. Janssen, and C. Goerick, "Task-oriented whole body motion for humanoid robots," in *IEEE-RAS*, 2005, pp. 238–244.

[5] L. Saab, O. E. Ramos, F. Keith, N. Mansard, P. Soueres, and J.-Y. Fourquet, "Dynamic whole-body motion generation under rigid contacts and other unilateral constraints," *IEEE Transactions on Robotics*, vol. 29, no. 2, pp. 346–362, 2013.

[6] V. Modugno, G. Neumann, E. Rueckert, G. Oriolo, J. Peters, and S. Ivaldi, "Learning soft task priorities for control of redundant robots," in *Robotics and Automation (ICRA), 2016 IEEE International Conference on*. IEEE, 2016, pp. 221–226.

[7] N. Hansen, S. Muller, and P. Koumoutsakos, "Reducing the time complexity of the derandomized evolution strategy with covariance matrix adaptation (CMA-ES)." *Evolutionary Computation*, vol. 11, no. 1, pp. 1–18, 2003.

[8] D. Wierstra, T. Schaul, J. Peters, and J. Schmidhuber, "Episodic reinforcement learning by logistic reward-weighted regression," in *International Conference on Artificial Neural Networks*. Springer, 2008, pp. 407–416.

[9] O. Kramer, A. Barthelmes, and G. Rudolph, "Surrogate constraint functions for cma evolution strategies." in *KI*. Springer, 2009, pp. 169–176.

[10] F. Sehnke, C. Osendorfer, T. Rückstieß, A. Graves, J. Peters, and J. Schmidhuber, "Parameter-exploring policy gradients," *Neural Networks*, vol. 23, no. 4, pp. 551–559, 2010.

[11] D. V. Arnold and N. Hansen, "A (1+ 1)-cma-es for constrained optimisation," in *Proceedings of the 14th annual conference on Genetic and evolutionary computation*. ACM, 2012, pp. 297–304.

[12] J. A. Bagnell and J. Schneider, "Covariant policy search," in *Proceedings of the 18th international joint conference on Artificial intelligence*. Morgan Kaufmann Publishers Inc., 2003, pp. 1019–1024.

[13] J. Peters, K. Mülling, and Y. Altün, "Relative entropy policy search," in *Proceedings of the Twenty-Fourth AAAI Conference on Artificial Intelligence*. AAAI Press, 2010, pp. 1607–1612.

[14] E. Rueckert, M. Mindt, J. Peters, and G. Neumann, "Robust policy updates for stochastic optimal control," in *Humanoid Robots (Humanoids), 2014 14th IEEE-RAS International Conference on*. IEEE, 2014, pp. 388–393.

[15] A. Abdolmaleki, R. Lioutikov, J. R. Peters, N. Lau, L. P. Reis, and G. Neumann, "Model-based relative entropy stochastic search," in *Advances in Neural Information Processing Systems*, 2015, pp. 3537–3545.

[16] E. Rueckert, G. Neumann, M. Toussaint, and W. Maass, "Learned graphical models for probabilistic planning provide a new class of movement primitives," *Frontiers in Computational Neuroscience*, vol. 6, no. 97, 2013. [Online]. Available: https://ai-lab.science/wp/Frontiers2013aRueckert.pdf, Article File

[17] R. B. Gramacy and H. K. Lee, "Optimization under unknown constraints," *arXiv preprint arXiv:1004.4027*, 2010.

[18] F. Berkenkamp, A. P. Schoellig, and A. Krause, "Safe controller optimization for quadrotors with gaussian processes," in *Robotics and Automation (ICRA), 2016 IEEE International Conference on*. IEEE, 2016, pp. 491–496.

[19] P. Englert and M. Toussaint, "Combined optimization and reinforcement learning for manipulation skills." in *Robotics: Science and Systems*, 2016.

[20] B. Shahriari, K. Swersky, Z. Wang, R. P. Adams, and N. de Freitas, "Taking the human out of the loop: A review of bayesian optimization," *Proceedings of the IEEE*, vol. 1, no. 104, pp. 148–175, 2016.

[21] B. Chen, R. Castro, and A. Krause, "Joint optimization and variable selection of high-dimensional gaussian processes," *arXiv preprint arXiv:1206.6396*, 2012.

[22] Z. Wang, M. Zoghi, F. Hutter, D. Matheson, and N. De Freitas, "Bayesian optimization in high dimensions via random embeddings," in *Twenty-Third International Joint Conference on Artificial Intelligence*, 2013.

[23] C. Li, S. Gupta, S. Rana, V. Nguyen, S. Venkatesh, and A. Shilton, "High dimensional bayesian optimization using dropout," *arXiv preprint arXiv:1802.05400*, 2018.

[24] S. Rana, C. Li, S. Gupta, V. Nguyen, and S. Venkatesh, "High dimensional bayesian optimization with elastic gaussian process," in *Proceedings of the 34th International Conference on Machine Learning-Volume 70*. JMLR. org, 2017, pp. 2883–2891.

[25] E. Rueckert, J. Camernik, J. Peters, and J. Babic, "Probabilistic movement models show that postural control precedes and predicts volitional motor control," *Nature Publishing Group: Scientific Reports*, vol. 6, no. 28455, 2016.

[26] R. Moriconi, K. Kumar, and M. P. Deisenroth, "High-dimensional bayesian optimization with manifold gaussian processes," *arXiv preprint arXiv:1902.10675*, 2019.

[27] D. J. Lizotte, T. Wang, M. H. Bowling, and D. Schuurmans, "Automatic gait optimization with gaussian process regression." in *IJCAI*, vol. 7, 2007, pp. 944–949.

[28] R. Martinez-Cantin, N. de Freitas, A. Doucet, and J. A. Castellanos, "Active policy learning for robot planning and exploration under uncertainty." in *Robotics: Science and Systems*, vol. 3, 2007, pp. 321–328.

[29] R. Calandra, A. Seyfarth, J. Peters, and M. P. Deisenroth, "Bayesian optimization for learning gaits under uncertainty," *Annals of Mathematics and Artificial Intelligence*, vol. 76, no. 1-2, pp. 5–23, 2016.

[30] C. K. Williams and C. E. Rasmussen, "Gaussian processes for regression," in *Advances in neural information processing systems*, 1996, pp. 514–520.

[31] ——, *Gaussian processes for machine learning*. MIT Press Cambridge, MA, 2006, vol. 2, no. 3.

[32] D. Nguyen-Tuong, M. Seeger, and J. Peters, "Model learning with local gaussian process regression," *Advanced Robotics*, vol. 23, no. 15, pp. 2015–2034, 2009.

[33] R. Calandra, S. Ivaldi, M. P. Deisenroth, E. Rueckert, and J. Peters, "Learning inverse dynamics models with contacts," in *2015 IEEE International Conference on Robotics and Automation (ICRA)*. IEEE, 2015, pp. 3186–3191.

[34] C. E. Rasmussen, "Gaussian processes in machine learning," in *Summer School on Machine Learning*. Springer, 2003, pp. 63–71.

[35] D. Nguyen-Tuong and J. Peters, "Model learning for robot control: a survey," *Cognitive processing*, vol. 12, no. 4, pp. 319–340, 2011.

[36] B. Matérn, "Spatial variation: Meddelanden fran statens skogsforskningsinstitut," *Lecture Notes in Statistics*, vol. 36, p. 21, 1960.

[37] M. Abramowitz and I. A. Stegun, *Handbook of mathematical functions: with formulas, graphs, and mathematical tables*. Courier Corporation, 1965, vol. 55.

[38] J. Mockus, V. Tiesis, and A. Zilinskas, "The application of bayesian methods for seeking the extremum," *Towards global optimization*, vol. 2, no. 117-129, p. 2, 1978.

[39] E. Nakano, H. Imamizu, R. Osu, Y. Uno, H. Gomi, T. Yoshioka, and M. Kawato, "Quantitative examinations of internal representations for arm trajectory planning: minimum commanded torque change model," *Journal of Neurophysiology*, vol. 81, no. 5, pp. 2140–2155, 1999.